Acta Crystallographica Section A
Foundations of Crystallography
ISSN 0108-7673

Received 23 October 2001
Accepted 15 January 2002

The asymptotic leading term of anisotropic small-angle scattering intensities. II. Non-convex particles

J.-M. Schneider,[a] S. Ciccariello,[b]* B Schönfeld[a] and G. Kostorz[a]

[a]ETH Zürich, Institut für Angewandte Physik, CH-8093 Zürich, Switzerland, and [b]Dipartimento di Fisica G. Galilei and sezione INFM, via F. Marzolo 8, I-35131 Padova, Italy. Correspondence e-mail: ciccariello@pd.infn.it

For anisotropic particulate samples with scattering contrast $(\Delta n)^2$, the leading asymptotic term of the scattering intensity, along a direction $\hat{\mathbf{q}}$ $(= \mathbf{q}/q)$ of reciprocal space, is $[4\pi^2(\Delta n)^2/q^4]\sum_j[1/|\kappa_{G,j}(\pm\hat{\mathbf{q}})|]$. Here, $\kappa_{G,j}(\pm\hat{\mathbf{q}})$ denotes the Gaussian curvature value at the points (labelled by j) of the interphase surface where the normal is either parallel or antiparallel to $\hat{\mathbf{q}}$. If the Gaussian curvature vanishes at, say, the $\bar{j}$th of these points, the corresponding contribution takes the form $\mathcal{C}_{\bar{j}}/q^{\alpha_{\bar{j}}}$ with $2 \leq \alpha_{\bar{j}} < 4$, $\mathcal{C}_{\bar{j}}$ and $\alpha_{\bar{j}}$ being determined by the local behaviour of the surface. However, the intensity detected by a counter pixel, with opening solid angle $\Delta\Omega(\hat{\mathbf{q}}_0)$ along (mean) direction $\hat{\mathbf{q}}_0$, asymptotically still behaves as $4\pi^2(\Delta n)^2 S(\Delta\Omega(\hat{\mathbf{q}}_0))/q^4$, where $S(\Delta\Omega(\hat{\mathbf{q}}_0))$ is the area of that part of the interface that has its normals inside $\Delta\Omega(\hat{\mathbf{q}}_0)$.

1. Introduction

Sample inhomogeneities occurring on a length scale of 1–1000 nm can usefully be investigated by small-angle scattering (SAS) of X-rays (Guinier & Fournet, 1955; Glatter & Kratky, 1982) and neutrons (Kostorz, 1996; Feigin & Svergun, 1987) as well as by light scattering (Lindner & Zemb, 1991). On this scale, samples can often be depicted as consisting of two homogeneous phases (Debye *et al.*, 1957). When absorption and inelastic effects are negligible, the scattering contrast $(\Delta n)^2$ is a real positive quantity and the wave vectors of incoming $(\mathbf{q}_{\rm in})$ and outgoing $(\mathbf{q}_{\rm out})$ radiation have equal modulus. Under these conditions, the scattering intensity $I(\mathbf{q})$ depends linearly on $(\Delta n)^2$ while its dependence on the scattering vector $\mathbf{q} \equiv (\mathbf{q}_{\rm in} - \mathbf{q}_{\rm out})$ is determined by the geometry of the interphase surface. Actually, only the points closer than $2\pi/q$ to the sample interfaces contribute to the scattering intensity [here, $q = (4\pi/\lambda)\sin(\theta/2)$ is the modulus of $\mathbf{q}$ while θ and λ denote the scattering angle and the wavelength of the incident radiation, respectively]. Since the thickness of these regions decreases as q increases, the asymptotic behaviour of the scattering intensity must depend on quantities related to the local behaviour of the interfaces. Porod's law (Porod, 1951*a*,*b*; Debye *et al.*, 1957) is a clear example of such a property. Since the derivation of this basic result, the relations existing between the asymptotic behaviour of the scattering intensity and the interface geometry were investigated in many papers. [For a brief review, see Ciccariello (1997).] These analyses were, however, confined to the case of statistically isotropic samples, where the observed intensity depends only on q. Nowadays, intensities can easily be registered by two-dimensional position-sensitive detectors, *i.e.* in dependence of $\mathbf{q}$, and anisotropic behaviour is frequently observed. Thus, it is worthwhile to look for a generalization of Porod's law to anisotropic samples. This problem was solved quite recently for the case of particulate samples with smooth and strictly convex particles (Ciccariello *et al.*, 2000). This paper, referred to as paper I hereinafter, showed that the Porod coefficient, *viz* the coefficient of the q^{-4} term, is proportional to the sum of the reciprocal Gaussian curvatures at all the points of the interface where the normals are either parallel or antiparallel to $\hat{\mathbf{q}} \equiv \mathbf{q}/q$, the direction of the considered scattering vector.

In the present paper, this result will be generalized to particles with non-convex surfaces. They may also include edges, vertices and planar facets. The paper is organized as follows. §2 shows that the leading asymptotic term of $I(\mathbf{q})$ is determined by the behaviour of the particle surfaces around those points – called $\hat{\mathbf{q}}$-tangency points – where the tangent planes are orthogonal to $\hat{\mathbf{q}}$. The three kinds of $\hat{\mathbf{q}}$-tangency points, *i.e.* elliptic, hyperbolic and parabolic, will be analysed in §§2.1, 2.2 and 2.3. §3 shows how to derive the leading asymptotic term of $I(\mathbf{q})$ from the results reported in §2. The changes required by the finiteness of experimental angular resolution are discussed in §4. Appendices *A* and *B* are devoted to some detailed applications.

2. General relations

When scattering is elastic, the scattering intensity $I(\mathbf{q})$ is the square modulus of the Fourier transform of $n(\mathbf{r})$, the scattering density (SD) function of the sample. For SAS, $n(\mathbf{r})$ can be identified with $\bar{n}(\mathbf{r})$, the average of $n(\mathbf{r})$ evaluated inside spheres with a radius of a few ångstroms. For most of the samples – noteworthy exceptions are fractal samples (Martin & Hurd, 1987), which will not be considered in the following – $\bar{n}(\mathbf{r})$ turns out to be fairly close to a discrete-valued function

(Debye *et al.*, 1957), denoted by $n_D(\mathbf{r})$ and sometimes referred to as Debye's idealized SD.[1] Denoting the values of $n_D(\mathbf{r})$ by $n_1, \ldots, n_N$, the sample regions where the SD is equal to n_j define the jth phase and the corresponding set, generally formed by disjoint sets with closed boundaries, will be denoted by $\mathcal{V}_j$.

We shall confine ourselves to particulate two-phase samples. Thus, consider a sample consisting of M particles and denote by V_p the sample region occupied by the pth particle. V_p is fully characterized by function $\rho_p(\mathbf{r})$, equal to one or zero depending on whether the tip of $\mathbf{r}$ lies inside or outside particle p. The sample region occupied by the particles is $\mathcal{V}_1 = \cup_{p=1}^{M} V_p$ and will be called phase 1. It is characterized by function $\rho_{\mathcal{V}_1}(\mathbf{r})$ given by

$$\rho_{\mathcal{V}_1}(\mathbf{r}) = \sum_{p=1}^{M} \rho_p(\mathbf{r}). \tag{1}$$

The sample region occupied by the medium where particles are immersed is denoted by $\mathcal{V}_2$ and forms phase 2. It is described by function $\rho_{\mathcal{V}_2}(\mathbf{r})$ with

$$\rho_{\mathcal{V}_2}(\mathbf{r}) = 1 - \rho_{\mathcal{V}_1}(\mathbf{r}). \tag{2}$$

If we denote the SD of phases 1 and 2 by n_1 and n_2, the SD function of the sample reads

$$n_D(\mathbf{r}) = n_1\rho_{\mathcal{V}_1}(\mathbf{r}) + n_2\rho_{\mathcal{V}_2}(\mathbf{r}) = \Delta n\rho_{\mathcal{V}_1}(\mathbf{r}) + n_2 \tag{3}$$

with the SD contrast $\Delta n = (n_1 - n_2)$. The scattering intensity is

$$I(\mathbf{q}) = |\mathcal{A}_D(\mathbf{q})|^2, \tag{4}$$

where $\mathcal{A}_D(\mathbf{q})$ is the scattering amplitude defined as

$$\mathcal{A}_D(\mathbf{q}) = \int \exp(i\mathbf{q}\cdot\mathbf{r})n_D(\mathbf{r})\,\mathrm{d}v. \tag{5}$$

Consider now the function

$$\mathcal{A}_p(\mathbf{q}) \equiv \int \exp(i\mathbf{q}\cdot\mathbf{r})\rho_p(\mathbf{r})\,\mathrm{d}v. \tag{6a}$$

It is fully determined by the geometry and the position of particle p, and will be called the geometrical scattering amplitude of particle p. Similarly, the geometrical scattering amplitude of phase 1 will be denoted by $\mathcal{A}_{\mathcal{V}_1}(\mathbf{q})$ and, owing to (1) and (6*a*), it reads

$$\mathcal{A}_{\mathcal{V}_1}(\mathbf{q}) = \sum_{p=1}^{M} \mathcal{A}_p(\mathbf{q}). \tag{6b}$$

For the scattering amplitude, one obtains

$$\mathcal{A}_D(\mathbf{q}) = (\Delta n)\mathcal{A}_{\mathcal{V}_1}(\mathbf{q}) + n_2(2\pi)^3\delta(\mathbf{q}), \tag{7}$$

where the Dirac function arises from assuming an infinitely large sample. After substitution of (7) in (4) and use of (6*b*), the scattering intensity becomes

$$I(\mathbf{q}) = (\Delta n)^2|\mathcal{A}_{\mathcal{V}_1}(\mathbf{q})|^2 = (\Delta n)^2\left|\sum_{p=1}^{M}\mathcal{A}_p(\mathbf{q})\right|^2, \quad \text{for} \quad \mathbf{q} \neq \mathbf{0}. \tag{8}$$

The intensity depends linearly on $(\Delta n)^2$, the scattering contrast. The shape of $I(\mathbf{q})$ is determined by the location and the geometry of the particles. As q increases, the asymptotic behaviour of $I(\mathbf{q})$ will be determined by *local* features of the interface between phases 1 and 2, as will be shown in the following. To this aim, it is however required that q is sufficiently large for the structure functions to be equal to one and, moreover, that the mean orientation of the particles inside the sample be approximately constant throughout the time interval required to collect the intensity. In the following, it will be assumed that these two conditons are fulfilled.

The asymptotic behaviour of $I(\mathbf{q})$ is immediately obtained by (8) once we have determined that of $\mathcal{A}_p(\mathbf{q})$, whatever p. With $\mathbf{r} = \xi\hat{\mathbf{q}} + \mathbf{r}_\perp$, $\xi \equiv (\hat{\mathbf{q}}\cdot\mathbf{r})$ and $\mathrm{d}v = \mathrm{d}\xi\mathrm{d}^2\mathbf{r}_\perp$, (6*a*) becomes

$$\mathcal{A}_p(q\hat{\mathbf{q}}) = \int_{-\infty}^{\infty} \mathrm{d}\xi\, \exp(iq\xi)A_p(\xi, \hat{\mathbf{q}}), \tag{9}$$

where

$$A_p(\xi, \hat{\mathbf{q}}) \equiv \int \rho_p(\xi\hat{\mathbf{q}} + \mathbf{r}_\perp)\,\mathrm{d}^2\mathbf{r}_\perp. \tag{10}$$

$A_p(\xi, \hat{\mathbf{q}})$ is the area of the intersection of particle p with $\Pi(\hat{\mathbf{q}}, \xi)$, the plane at distance ξ from the origin and orthogonal to $\hat{\mathbf{q}}$. According to a general theorem (Erdélyi, 1958) on Fourier transforms (FT), the behaviour of $\mathcal{A}_p(q\hat{\mathbf{q}})$ at large q values is determined by the continuity properties of $A_p(\xi, \hat{\mathbf{q}})$. Equation (10) shows that these depend on the shape of the particle. In contrast to paper I, particles are no longer required to be convex. They must only have finite sizes and smooth boundaries except for possible edges and vertices. The complications arising from these more general conditions are discussed by referring to the particle shown in Fig. 1. It is a

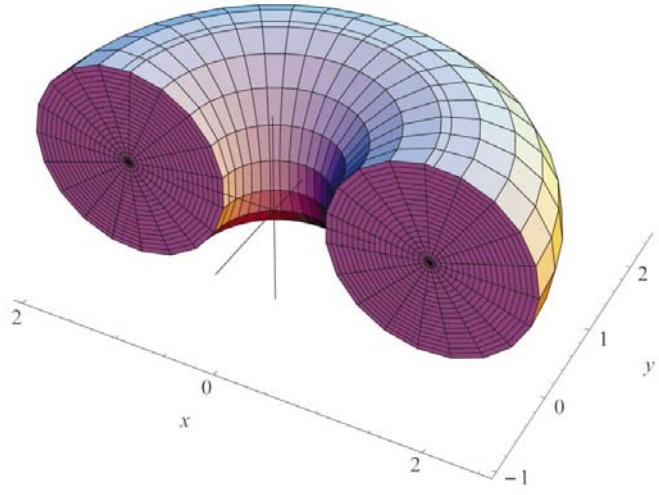

Figure 1
A half-torus with radii $R_0 = 1$ and $R_1 = 1.5$. The points P_H and P_E, referred to in the text, are the first and the second intersections of axis y with the toroidal surface, respectively. In particular, P_E lies behind the surface.

[1] Actually, $n_D(\mathbf{r})$ differs from the true SD both at the phase borders and inside the phases. The first deviation arises from the fact that the true SD changes continuously in passing from one phase to another; it can be accounted for by Ruland's procedure (Ruland, 1971). The second deviation is corrected by subtracting the so-called background contribution (Luzzati *et al.*, 1961).

half-torus, denoted by $\mathcal{T}$, with radii R_0 and R_1, R_1 being greater than R_0. [The complete torus has its centre of symmetry at the origin and its C_∞ axis along z.] The surface of $\mathcal{T}$ has two circular edges, with radius R_0 and the centres at $(\pm R_1, 0, 0)$. Consider direction $\hat{\mathbf{q}}_1 = (0, 1, 0)$. Plane $\Pi(\hat{\mathbf{q}}_1, \xi)$ intersects $\mathcal{T}$ only if $0 \leq \xi \leq (R_0 + R_1)$. Thus, $A_{\mathcal{T}}(\xi, \hat{\mathbf{q}}) = 0$ if $\xi < 0$ or if $\xi > (R_0 + R_1)$. In the range $0 \leq \xi \leq (R_0 + R_1)$, $A_{\mathcal{T}}(\xi, \hat{\mathbf{q}})$ changes continuously with ξ and consists of two disjoint sets if $0 \leq \xi < (R_1 - R_0)$, which join each other at $\xi = (R_1 - R_0)$ (see Fig. 2*a*). In the remaining interval $[(R_1 - R_0), (R_1 + R_0)]$, $A_{\mathcal{T}}(\xi, \hat{\mathbf{q}})$ is a set that shrinks to a point as $\xi \rightarrow (R_1 + R_0)$ (see Fig. 2*b*). Thus, $A_{\mathcal{T}}(\xi, \hat{\mathbf{q}})$ is a continuous function of ξ except for $\xi = 0$ where it has a finite discontinuity. Finite discontinuities of $A_p(\xi, \hat{\mathbf{q}})$ are present only if the particle surface contains planar subsets orthogonal to $\hat{\mathbf{q}}$. If we denote the areas of these planar subsets by $S_1(\hat{\mathbf{q}}), \ldots, S_s(\hat{\mathbf{q}})$ and their distances from the origin by $\delta_1, \ldots, \delta_s$, the discontinuity at the jth of these ξ values is

$$A_p(\delta_j^+, \hat{\mathbf{q}}) - A_p(\delta_j^-, \hat{\mathbf{q}}) = -(\hat{\mathbf{v}}_j \cdot \hat{\mathbf{q}}) S_j(\mathbf{q}), \tag{11}$$

where $\hat{\mathbf{v}}_j$ denotes the unit normal to the jth planar set of the particle surface, pointing out of the particle. [Note that $\hat{\mathbf{v}}_j \cdot \hat{\mathbf{q}}$ in (11) is equal to either $+1$ or -1.] It is convenient to write (10) as

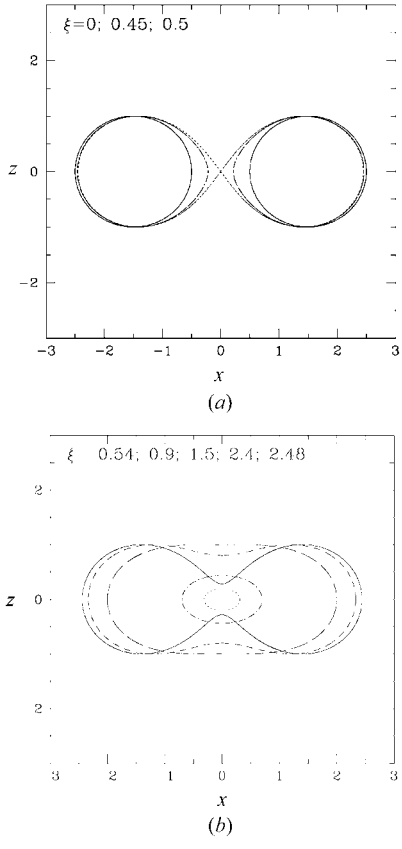

Figure 2
The curves shown are the sections of the surface depicted in Fig. 1 with the planes orthogonal to axis y at the distances ξ given at the top of each figure. The cross point of the curve relevant to $\xi = 0.5$ in (*a*) represents point P_H, while the ellipsoidal curves shown in (*b*) shrink towards P_E as $\xi \rightarrow 2.5$.

$$A_p(\xi, \hat{\mathbf{q}}) = \int \rho_p(\mathbf{r}) \delta(\mathbf{r} \cdot \hat{\mathbf{q}} - \xi)\, \mathrm{d}v, \tag{12}$$

where the presence of the Dirac δ function ensures that only the points lying on $\Pi(\hat{\mathbf{q}}, \xi)$ contribute to the integral. The ξ derivatives of $A_p(\xi, \hat{\mathbf{q}})$, considered as distributions, can be evaluated by taking the ξ derivatives of the integrand (Guelfand & Chilov, 1962). Thus, by the identity

$$\frac{\mathrm{d}\delta(\mathbf{r} \cdot \hat{\mathbf{q}} - \xi)}{\mathrm{d}\xi} = -(\hat{\mathbf{q}} \cdot \nabla)\delta(\mathbf{r} \cdot \hat{\mathbf{q}} - \xi) = -\nabla \cdot [\hat{\mathbf{q}} \delta(\mathbf{r} \cdot \hat{\mathbf{q}} - \xi)]$$

and by the Gauss theorem, one finds

$$A'_p(\xi, \hat{\mathbf{q}}) = -\int_{\Sigma_p} \mathrm{d}S\, (\hat{\mathbf{v}} \cdot \hat{\mathbf{q}}) \delta(\mathbf{r} \cdot \hat{\mathbf{q}} - \xi), \tag{13}$$

where the integral is performed over the particle surface Σ_p, and $\hat{\mathbf{v}}$ is the unit vector orthogonal to dS. At a discontinuity point, say δ_j, the contribution of subset S_j (orthogonal to $\hat{\mathbf{q}}$) is immediately evaluated because the δ function can be taken out of the integral since its argument is constant on S_j. One finds

$$A'_p(\xi, \hat{\mathbf{q}}) = -\sum_{j=1}^{s} (\hat{\mathbf{v}}_j \cdot \hat{\mathbf{q}}) S_j \delta(\xi - \delta_j) + A'_{p,C}(\xi, \hat{\mathbf{q}}) \tag{14}$$

with

$$A'_{p,C}(\xi, \hat{\mathbf{q}}) \equiv -\int_{\Sigma'_p} \mathrm{d}S\, (\hat{\mathbf{v}} \cdot \hat{\mathbf{q}}) \delta(\mathbf{r} \cdot \hat{\mathbf{q}} - \xi), \tag{15}$$

where Σ'_p [$\equiv \Sigma_p \backslash \{\cup_{j=1}^{s} S_j\}$] denotes the particle surface without the planar facets orthogonal to $\hat{\mathbf{q}}$. Integrating (9) by parts and using (14), one gets

$$A_p(q\hat{\mathbf{q}}) = (1/iq) \sum_{j=1}^{s} \exp(iq\delta_j)(\hat{\mathbf{v}}_j \cdot \hat{\mathbf{q}}) S_j + (1/iq) \int_{-\infty}^{\infty} \mathrm{d}\xi\, \exp(iq\xi) A'_{p,C}(\xi, \hat{\mathbf{q}}). \tag{16}$$

Hence, possible planar subsets of the particle surface, which are orthogonal to $\hat{\mathbf{q}}$, yield $O(q^{-1})$ asymptotic contributions to the scattering amplitude along direction $\hat{\mathbf{q}}$ in reciprocal space.

To find the asymptotic behaviour of the remaining integral on the right-hand side (r.h.s.) of (16), we must study the continuity properties of $A'_{p,C}(\xi, \hat{\mathbf{q}})$ with respect to ξ. In (15), the δ function restricts the integral to the points of Σ'_p, which lie on $\Pi(\hat{\mathbf{q}}, \xi)$, while Σ'_p, by definition, no longer contains the planar subsets of the particle surface. Thus, the intersection of Σ'_p with $\Pi(\hat{\mathbf{q}}, \xi)$, if it exists, can only be a curve denoted by $\Gamma(\xi, \hat{\mathbf{q}})$, which may consist of disjoint arcs. For simplicity, we proceed as if $\Gamma(\xi, \hat{\mathbf{q}})$ consists of a single arc. In this case, integral (15) reduces to a curvilinear integral along $\Gamma(\xi, \hat{\mathbf{q}})$. Owing to the Dirac δ function, the integrand of (15) is certainly continuous at the points of $\Gamma(\xi, \hat{\mathbf{q}})$ where the normal to the infinitesimal surface element dS is not parallel to $\hat{\mathbf{q}}$ (Guelfand & Chilov, 1962). Thus, the evaluation of (15) requires some care only around the points of $\Gamma(\xi, \hat{\mathbf{q}})$, which are $\hat{\mathbf{q}}$ tangency points. In fact, these points can make the behaviour of $A'_{p,C}(\xi, \hat{\mathbf{q}})$ discontinuous as $\xi \rightarrow \delta_i$, δ_i denoting the distance of the plane, tangent to the particle surface at one of these points, from the origin. To understand the phenomena

occurring around such points, we refer again to Fig. 1. Here, points P_H and P_E denote the two $\hat{\mathbf{q}}_1$ tangency points for $\hat{\mathbf{q}}_1 = (0, 1, 0)$. Their distances from the origin are $(R_1 - R_0)$ and $(R_0 + R_1)$. Put now $\delta_1 = (R_1 + R_0)$ and $\delta_2 = (R_1 - R_0)$. Around P_E, $\Gamma(\xi, \hat{\mathbf{q}})$ exists only if $\xi < \delta_1$ and it shrinks to a point as $\xi \to \delta_1^-$. Thus, in this limit, the integration domain goes to zero, but the integrand diverges as the normal to dS becomes parallel to $\hat{\mathbf{q}}$. In §2.1, it will be shown that, provided the Gaussian curvature of the particle surface at P_E be greater than zero, the opposite behaviours of the integration domain and of the integrand combine to give a finite limit for $A'_{p,C}(\xi, \hat{\mathbf{q}})$ as $\xi \to \delta_1^-$. Thus, $A'_{p,C}(\xi, \hat{\mathbf{q}})$ has a finite discontinuity at $\xi = \delta_1$. Around P_H, $\Gamma(\xi, \hat{\mathbf{q}})$ exists in a complete neighbourhood of δ_2. In fact, for $\xi < \delta_2$, $\Gamma(\xi, \hat{\mathbf{q}})$ consists of two disjoint closed curves which merge into a single curve, presenting the cross point P_H, at $\xi = \delta_2$ (see Fig. 2*a*). As $\xi \to \delta_2{}^+$, $\Gamma(\xi, \hat{\mathbf{q}})$ consists of a single closed curve which develops a cross point at $\xi = \delta_2$. Then, in both cases, the integration domain remains finite and the singularity of the integrand, under the assumption that the Gaussian curvature is smaller than zero, yields a logarithmic singularity for $A'_{p,C}(\xi, \hat{\mathbf{q}})$ as $\xi \to \delta_2$, as shown in §2.2. According to mathematical nomenclature, a point P of a surface is called elliptic, hyperbolic or parabolic depending on whether the Gaussian curvature, denoted by $\kappa_G(P)$, is greater, smaller or equal to zero (Smirnov, 1970). If $\kappa_G(P) > 0$, the plane tangent to the surface at P lies on one side of the surface as in the case of point P_E. If $\kappa_G(P) < 0$, the plane tangent to the surface at P cuts the surface as in the P_H case. If $\kappa_G(P) = 0$, the tangent plane can either cut or lie on one side of the surface.

2.1. Elliptic $\hat{\mathbf{q}}$ tangency point

This case was discussed in paper I. We shall generalize it to the case of a particle surface with edges. Consider first an elliptic $\hat{\mathbf{q}}$ tangency point P_E that does not lie on an edge and assume, for definiteness, that $\hat{\mathbf{v}}_{P_E} = +\hat{\mathbf{q}}$, $\hat{\mathbf{v}}_{P_E}$ denoting the normal to Σ'_p at P_E. Then, $\Gamma(\xi, \hat{\mathbf{q}})$ exists only for $\xi \to \delta^-$ so that $A'_{p,C}(\xi, \hat{\mathbf{q}}) = 0$ for $\xi > \delta$. Using the same procedure as followed in paper I to get (10), one finds with $\xi \to \delta^-$

$$A'_{p,C}(\xi, \hat{\mathbf{q}}) = -2\pi/[\kappa_G(P_E)]^{1/2} + o. \qquad (17)$$

Here, o denotes a contribution approaching zero as $\xi \to \delta^-$ and $\kappa_G(P_E)$ is the value of the Gaussian curvature of the particle surface at P_E. In a neighbourhood of δ, one can write

$$A'_{p,C}(\xi, \hat{\mathbf{q}}) = \Theta[(\hat{\mathbf{v}}_{P_E} \cdot \hat{\mathbf{q}})(-\xi)]\{-2\pi/[\kappa_G(P_E)]^{1/2} + o\}, \qquad (18)$$

where Θ is the Heaviside step function. Equation (18) shows that $A'_{p,C}(\xi, \hat{\mathbf{q}})$ presents a finite discontinuity at $\xi = \delta$. By the theorem reported by Erdélyi (1958, §2.8), this singularity contributes to the leading asymptotic behaviour of the FT on the r.h.s. of (16) with

$$\{2\pi/[\kappa_G(P_E)]^{1/2}\}[\exp(iq\delta)/q^2]. \qquad (19)$$

If $\hat{\mathbf{v}}_{P_E} = -\hat{\mathbf{q}}$, $\Gamma(\xi, \hat{\mathbf{q}})$ exists only for $\xi > \delta$ and $A'_{p,C}(\xi, \hat{\mathbf{q}})$ still behaves as reported on the r.h.s. of (18). With $\hat{\mathbf{v}}_{P_E} \cdot \hat{\mathbf{q}} = -1$, the leading term of the FT on the r.h.s. of (16) will be equal to (19) with a negative sign. Combining both results, one concludes that the leading contribution of an elliptic $\hat{\mathbf{q}}$ tangency point to the asymptotic behaviour of the scattering amplitude is

$$A_p(q\hat{\mathbf{q}}) \approx \{[2\pi(\hat{\mathbf{v}}_{P_E} \cdot \hat{\mathbf{q}})]/[\kappa_G(P_E)]^{1/2}\}[\exp(iq\delta)/q^2]. \qquad (20)$$

We now consider the case where the particle surface presents an edge. The equation of the particle surface at the left of the edge is different from that at the right, so that one can speak of a left and a right branch of the particle surface. Assume now that P_E is an elliptic $\hat{\mathbf{q}}$ tangency point for one of the surface branches (say the left one) and that it lies on the edge. In order to evaluate the behaviour of $A'_{p,C}(\xi, \hat{\mathbf{q}})$ as $\xi \to \delta$, we must only analyse the contribution due to the left branch of the surface. Close to P_E, a portion of $\Gamma(\xi, \hat{\mathbf{q}})$ will lie on the left surface only if $\xi > \delta$ or if $\xi < \delta$. For definiteness, assume that this occurs for $\xi < \delta$. The considered portion of $\Gamma(\xi, \hat{\mathbf{q}})$ is an open curve. Thus, each of its two ends determines a curve as $\xi \to \delta^-$, and the two curves meet each other at P_E. Consider now the tangent to each curve at point P_E. (Depending on the chosen curve, the tangent will be defined by a right or left limit.) The two tangents will form an angle, denoted by α, such that $0 < \alpha < 2\pi$. If we remember that the factor 2π in (18) arises from the integration along a closed contour shrinking to a point as $\xi \to \delta^-$, it is clear that an elliptic $\hat{\mathbf{q}}$ tangency point lying on an edge and the associated surface branch contribute to the leading asymptotic scattering amplitude as in (20) provided 2π is substituted by α and $\kappa_G(P_E)$ refers to the considered branch of the surface.

2.2. Hyperbolic $\hat{\mathbf{q}}$ tangency point

The discussion of this case is more involved than the elliptic one because the length of $\Gamma(\xi, \hat{\mathbf{q}})$ does not go to zero as one approaches P_H. If $\xi \neq \delta$, the contribution to $A'_{p,C}(\xi, \hat{\mathbf{q}})$ from the $\Gamma(\xi, \hat{\mathbf{q}})$ part within a small neighbourhood of P_H exists and is finite. It will be shown that, as $\xi \to \delta$, this contribution behaves as $\mathcal{C} \ln|\xi - \delta|$, $\mathcal{C}$ being an appropriate coefficient. Similarly to paper I, consider the orthogonal Cartesian frame $OXYZ$ with axis Z along $\hat{\mathbf{q}}$ and axes X and Y along the principal curvature directions of Σ'_p at P_H. In this system, the coordinates of $\hat{\mathbf{q}}$ and P_H are $(0, 0, 1)$ and (X_H, Y_H, δ), while the parametric equation of Σ'_p around P_H becomes $Z = Z(X, Y)$ with $Z(X_H, Y_H) = \delta$. Besides, the local approximation of Σ'_p by its osculating quadric, obtained by expanding $Z(X, Y)$ around P_H up to second-order terms, is

$$Z \approx \delta + (au^2 + bv^2)/2. \qquad (21)$$

Here we have put $u = X - X_H$, $v = Y - Y_H$, $a = \partial^2 Z(X, Y)/\partial X^2|$, $b = \partial^2 Z(X, Y)/\partial Y^2|$, and the vertical bars mean that the derivatives are evaluated at P_H. [In (21), the first-order derivatives and the mixed second derivative are not present because the plane tangent to Σ'_p at P_H is parallel to plane XY and because axes X and Y point along the principal curvature directions.] The value of the Gaussian curvature at P_H is $\kappa_G(P_H) = ab$ and, by assumption, it is negative. Thus, either $a > 0$ and $b < 0$ or $a < 0$ and $b > 0$. For definiteness, we

consider the first case. Referring to frame $OXYZ$ and using the local coordinates (u, v) defined above, we can write the parametric equations of Σ'_p as $\mathbf{r} = \mathbf{r}(u, v)$, with $x = u + X_H$, $y = v + Y_H$ and $z = \delta + (au^2 + bv^2)/2$, in a neighbourhood of P_H sufficiently small to use (21). By well known formulae of differential geometry (Smirnov, 1970), one has

$$dS = (EG - F^2)^{1/2}\, du\, dv, \tag{22a}$$

$$\hat{\boldsymbol{\nu}} = (\mathbf{r}_u \times \mathbf{r}_v)/(EG - F^2)^{1/2}, \tag{22b}$$

where

$$\mathbf{r}_u \equiv \partial\mathbf{r}/\partial u = (1, 0, au), \quad \mathbf{r}_v \equiv \partial\mathbf{r}/\partial v = (0, 1, bv),$$
$$E \equiv \mathbf{r}_u \cdot \mathbf{r}_u = 1 + a^2u^2, \quad F \equiv \mathbf{r}_u \cdot \mathbf{r}_v = abuv,$$
$$G \equiv \mathbf{r}_v \cdot \mathbf{r}_v = 1 + b^2v^2.$$

After putting

$$\zeta \equiv \delta - \xi, \tag{22c}$$

one has

$$\Xi \equiv \mathbf{r}(u, v) \cdot \hat{\mathbf{q}} - \xi = \zeta - (au^2 + bv^2)/2. \tag{22d}$$

The contribution to $A'_{p,C}(\xi, \hat{\mathbf{q}})$ [defined by (15)] from the part of $\Gamma(\xi, \hat{\mathbf{q}})$ that lies inside the considered neighbourhood of P_H becomes

$$A'_{p,C}(\xi, \hat{\mathbf{q}}) = -\int [(\mathbf{r}_u \times \mathbf{r}_v) \cdot \hat{\mathbf{q}}]\delta(\Xi)\, du\, dv. \tag{23}$$

Define new variables $\bar{u} = u(a/2)^{1/2}$ and $\bar{v} = v(-b/2)^{1/2}$. Depending on whether $\zeta > 0$ or $\zeta < 0$, Ξ factorizes either as $\Xi = [(\zeta + \bar{v}^2)^{1/2} - \bar{u}][(\zeta + \bar{v}^2)^{1/2} + \bar{u}]$ or as $\Xi = [(-\zeta + \bar{u}^2)^{1/2} - \bar{v}][(-\zeta + \bar{u}^2)^{1/2} + \bar{v}]$, so as to have positive radicals in both cases. Consider the case $\zeta > 0$. One has the identity

$$\delta(\Xi) = \frac{1}{2(\zeta + \bar{v}^2)^{1/2}}\{\delta[(\zeta + \bar{v}^2)^{1/2} - \bar{u}] + \delta[(\zeta + \bar{v}^2)^{1/2} + \bar{u}]\} \tag{24}$$

and (23) becomes

$$A'_{p,C}(\xi, \hat{\mathbf{q}}) = -\frac{2}{(-ab)^{1/2}} \int_{-L}^{L} \left[\frac{(\mathbf{r}_u \times \mathbf{r}_v) \cdot \hat{\mathbf{q}}}{2(\zeta + \bar{v}^2)^{1/2}} \right|_+ + \left. \frac{(\mathbf{r}_u \times \mathbf{r}_v) \cdot \hat{\mathbf{q}}}{2(\zeta + \bar{v}^2)^{1/2}} \right|_- \Bigg] d\bar{v}, \tag{25a}$$

where the first and second vertical bars mean that the numerators are evaluated at $\bar{u} = (\zeta + \bar{v}^2)^{1/2}$ and at $\bar{u} = -(\zeta + \bar{v}^2)^{1/2}$, respectively. Besides, the integration limit L is chosen so as to have a finite subset of $\Gamma(\xi, \hat{\mathbf{q}})$ within the considered neighbourhood of P_H. It will be shown below that the exact value of L is not important. From the relations reported above (22c), it follows that $\hat{\mathbf{q}} \cdot (\mathbf{r}_u \times \mathbf{r}_v) = -1$ aside from an infinitesimal correction. Hence, the two terms inside the integrand are equal and integral (25a) is easily evaluated. Its value is

$$2(-ab)^{1/2} \ln\{[(\zeta + L^2)^{1/2} + L]/[(\zeta + L^2)^{1/2} - L]\}. \tag{25b}$$

Since $\zeta \to 0^+$, the leading term is $-2(-ab)^{1/2} \ln \zeta$, which, as noted above, is independent of L. As $\zeta \to 0^-$, one considers the second factorization for Ξ. After performing the changes $\zeta \to -\zeta$, $\bar{u} \to \bar{v}$ and $\bar{v} \to \bar{u}$ in (24), by the same analysis reported above one finds that the leading term of (23), as $\zeta \to 0^-$, is $-2(-ab)^{1/2} \ln(-\zeta)$. In conclusion, the leading term of (23), as one approaches P_H from the left or from the right, is

$$A'_{p,C}(\xi, \hat{\mathbf{q}}) \approx -2|\kappa_G(P_H)|^{-1/2} \ln(|\xi - \delta|), \tag{26}$$

which, as already anticipated, is logarithmically singular. The leading asymptotic term of the FT of this contribution has been obtained by Erdélyi (1955) and by Jones & Kline (1958). Using theorems 1 and 2 reported in the Appendix of the latter paper, one finds that the leading asymptotic contribution, generated by a hyperbolic $\hat{\mathbf{q}}$ tangency point, to the scattering amplitude is

$$A_p(q\hat{\mathbf{q}}) \approx -\frac{i2\pi}{|\kappa_G(P_H)|^{1/2}} \frac{\exp(iq\delta)}{q^2}. \tag{27}$$

The geometrical meaning of equation $\Xi = 0$, with Ξ given by (22d), is as follows. Both for $\zeta < 0$ and for $\zeta > 0$, equation $\Xi = 0$ represents the two branches of a hyperbola which approximates the intersection curve $\Gamma(\xi, \hat{\mathbf{q}})$ close to P_H and approaches its asymptotes as $\zeta \to 0^{\pm}$. This appears evident by looking at Fig. 2, where the sections of $\mathcal{T}$ with some planes, orthogonal to $\hat{\mathbf{q}} = (0, 1, 0)$ and set at different distances (ξ) from the origin, are shown. Point P_H is the cross point of the dotted curve shown in Fig. 2(a), and its coordinates are $(0, 0.5, 0)$. Consider the dashed-dotted curve of Fig. 2(a) and the continuous curve of Fig. 2(b). They were obtained by taking $\xi = 0.45$ and $\xi = 0.54$, respectivley. Clearly, both curves are close to a hyperbola only near P_H. Inside a small neighbourhood of P_H, one finds that, as $\xi \to 0.5^{\pm}$ (or $\zeta \to 0^{\pm}$), the intersection curves become closer to hyperbola $\Xi = 0$, which in turn approaches its asymptotes. In fact, the dotted curve shown in Fig. 2(a) refers to $\zeta = 0$ and, around P_H, it is made up of two intersecting straight lines. It is also noted that each of the two integrals on the r.h.s. of (25a) corresponds to an integration over one branch of the hyperbola, *i.e.* the left or the right branch if $\zeta < 0$, or the upper or the lower branch if $\zeta > 0$. In any case, one integrates over that part of the branch that lies inside the considered neighbourhood of P_H. Moreover, the first integral on the r.h.s. of (25a) can be written as

$$\int_{-L}^{L} \left. \frac{(\mathbf{r}_u \times \mathbf{r}_v) \cdot \hat{\mathbf{q}}}{2(\zeta + \bar{v}^2)^{1/2}} \right|_+ d\bar{v} = \int_{-L}^{0} \left. \frac{(\mathbf{r}_u \times \mathbf{r}_v) \cdot \hat{\mathbf{q}}}{2(\zeta + \bar{v}^2)^{1/2}} \right|_+ d\bar{v} + \int_{0}^{L} \left. \frac{(\mathbf{r}_u \times \mathbf{r}_v) \cdot \hat{\mathbf{q}}}{2(\zeta + \bar{v}^2)^{1/2}} \right|_+ d\bar{v}.$$

The two integrals on the r.h.s. are equal. As $\zeta \to 0$, each of them tends to the integral over that part of the relevant asymptote which goes from P_H to the border of the considered neighbourhood of P_H. The previous remarks also apply to the second integral present on the r.h.s. of (25a) and make the evaluation of the contribution arising from a hyperbolic $\hat{\mathbf{q}}$ tangency point, lying on an edge of the particle surface, straightforward. After orienting the edge, denote the parts of the particle surface lying on the left and on the right of the edge by Σ_L and Σ_R, respectively. Assume, for definiteness,

that P_H be a hyperbolic point of Σ_R. Consider now the plane tangent to Σ_R at P_H, and the straight line tangent to the edge at P_H and oriented as the edge. This oriented straight line divides the tangent plane into a left and a right half-plane. The asymptotes of the hyperbola lie in the aforesaid tangent plane. In the limit $\zeta \to 0$, we must consider only those parts of the asymptotes that lie on the right half-plane and in a neighbourhood of P_H. Leaving aside the exceptional case where the aforesaid straight line coincides with one asymptote, the tangent half-plane only contains two half-asymptotes. Therefore, the leading contributions to $A'_{p,C}(\xi, \hat{\mathbf{q}})$ and $A_p(q\hat{\mathbf{q}})$ are those given by (26) and (27), divided by two.

2.3. Parabolic $\hat{\mathbf{q}}$ tangency point

By definition, this is a point, denoted by P_P, of the surface where the normal is equal to $\pm\hat{\mathbf{q}}$ and the Gaussian curvature is equal to zero, *i.e.* $\kappa_G(P_P) = 0$. The distance from the origin to the plane tangent to the surface at P_P will still be denoted by δ, and we shall refer to a Cartesian frame $OXYZ$ defined as in the previous subsections. The parametric equation of Σ'_p can be written as $Z = Z(X, Y)$ in a neighbourhood of $P_P \equiv (X_P, Y_P, \delta)$. Expanding $Z(X, Y)$ around this point, one finds

$$\mathbf{r}\cdot\hat{\mathbf{q}} \approx -a|X - X_P|^{\alpha} - b|Y - Y_P|^{\beta} - c|X - X_P|^{\alpha_1}|Y - Y_P|^{\beta_1}, \tag{28a}$$

assuming that Σ'_p lies on one side of its tangent plane $\Pi(\hat{\mathbf{q}}, \delta)$ at P_P. Exponents α, β, α_1 and β_1 are subject to constraints

$$\alpha \geq 2, \quad \beta \geq 2, \quad \alpha + \beta > 4 \tag{28b-d}$$

$$\alpha_1 \geq 2, \quad \beta_1 \geq 2. \tag{28e-f}$$

These constraints follow from the properties that the plane tangent to Σ'_p at P_P be orthogonal to $\hat{\mathbf{q}}$, that $Z(X, Y)$ be a C^2 function and that $\kappa_G(P_P) = 0$. As $\xi \to \delta$, the behaviour of integral (15) depends on the values of the exponents and of the coefficients in (28*a*). Only two of the simplest cases will now be discussed since these results will be used later on. This discussion also shows how to handle other cases.

Our first example deals with the case where the equation of Σ'_p depends only on one variable so that, in a neighbourhood of P_P, it can be written as $Z = Z(X)$. This is the case of a cylinder resulting from the translation along Y of a closed curve described by the equation $F(X, Z) = 0$. Besides, we assume that the cylinder at $P_P = (0, Y_P, \delta)$ has $\hat{\boldsymbol{\nu}} = \hat{\mathbf{q}} = (0, 0, 1)$. By expanding around P_P, one gets

$$\mathbf{r}\cdot\hat{\mathbf{q}} \approx \delta(1 - a|X/\delta|^{\alpha} + o) \quad \text{with} \quad \alpha \geq 2.$$

(For instance, in the case of right circular cylinders with radius δ, one has $a = 1/2$ and $\alpha = 2$.) Using definition (22*c*), the argument of the Dirac δ function in (15) becomes

$$\Xi = \mathbf{r}\cdot\hat{\mathbf{q}} - \xi \approx \zeta - a\delta|X/\delta|^{\alpha}. \tag{29a}$$

The Dirac δ function requires that $\Xi = 0$. The solutions of this equation are

$$X = \pm\delta(\zeta/a\delta)^{1/\alpha} + o. \tag{29b}$$

They make sense provided $\zeta/a > 0$. Thus, $A'_{p,C}(\xi, \hat{\mathbf{q}})$ exists only if $\zeta > 0$ or if $\zeta < 0$, depending on whether $a > 0$ or $a < 0$, respectively. For definiteness, we consider the case $a > 0$. We denote the height and the Y coordinate of the centre of the cylinder by H and Y_0, respectively, and we put $u = X$ and $v = Y + Y_0$ in (23). As $\zeta \to 0^+$, one has $(\mathbf{r}_u \times \mathbf{r}_v)\cdot\hat{\mathbf{q}} \to 1$, and (15) becomes

$$A'_{p,C}(\xi, \hat{\mathbf{q}}) \approx -\int_{-H/2}^{H/2} \mathrm{d}Y \int \delta(\Xi)\left|\frac{\mathrm{d}X}{\mathrm{d}\Xi}\right| \mathrm{d}\Xi = -2\int_{-H/2}^{H/2}\left|\frac{\mathrm{d}X}{\mathrm{d}\Xi}\right|_{+} \mathrm{d}Y. \tag{29c}$$

The factor 2 in the last expression accounts for the fact that the Jacobian $|\mathrm{d}X/\mathrm{d}\Xi|$ takes the same value at the two roots (29*b*) of equation $\Xi = 0$. By (29*a*), equation (29*c*) becomes

$$A'_{p,C}(\xi, \hat{\mathbf{q}}) \approx -\frac{2H\Theta(a\zeta)}{\alpha|a|^{1/\alpha}}\left(\frac{\delta}{|\zeta|}\right)^{(\alpha-1)/\alpha}, \tag{30}$$

where the absolute value of a makes (30) valid also when $a < 0$.

Our second example is the case where the expansion of $Z(X, Y)$, given by (28*a*), has $2 \leq \alpha \leq \beta$, $ab > 0$ and $c = 0$. For definiteness, it will be assumed that $a > 0$ and $b > 0$. The Ξ expression is

$$\Xi \approx \zeta - a|u|^{\alpha} - b|v|^{\beta}, \tag{31}$$

with $u = X - X_P$, $v = Y - Y_P$ and $\zeta = \delta - \xi$. The roots of the equation $\Xi = 0$ are

$$u = \pm[(\zeta - b|v|^{\beta})/a]^{1/\alpha}. \tag{32a}$$

For these to exist, v has to obey

$$|v| \leq (\zeta/b)^{1/\beta}. \tag{32b}$$

This implies that $A'_{p,C}(\xi, \hat{\mathbf{q}})$ can differ from zero only if $b\zeta > 0$. Similar to (29*c*), integral (23) becomes

$$A'_{p,C}(\xi, \hat{\mathbf{q}}) \approx -2\int\left|\frac{\mathrm{d}u}{\mathrm{d}\Xi}\right|_{+} \mathrm{d}v.$$

From (31), one gets $|\mathrm{d}u/\mathrm{d}\Xi| = 1/(a\alpha|u|^{\alpha-1})$. Using constraint (32*b*) and putting $v = (\zeta/b)^{1/\beta}\tau$, the previous integral becomes

$$A'_{p,C}(\xi, \hat{\mathbf{q}}) \approx -\frac{4}{\alpha a^{1/\alpha} b^{1/\beta} \zeta^{1-1/\alpha-1/\beta}} \int_0^1 [1 - \tau^{\beta}]^{(1-\alpha)/\alpha}\, \mathrm{d}\tau.$$

This can be integrated (Gradshtein & Ryzhik, 1980, equation 3.251.1) in terms of Euler's Γ function. The final result is

$$A'_{p,C}(\xi, \hat{\mathbf{q}}) \approx -\frac{4\Theta(a\zeta)\Gamma(1/\alpha)\Gamma(1/\beta)}{\alpha\beta|a|^{1/\alpha}|b|^{1/\beta}\Gamma(1/\alpha + 1/\beta)|\zeta|^{1-1/\alpha-1/\beta}}, \tag{33}$$

which also applies when both a and b are negative.

3. Asymptotic behaviour of the scattering intensity

In the previous section, it has been shown that, around a $\hat{\mathbf{q}}$ tangency point, $A'_{p,C}(\xi, \hat{\mathbf{q}})$ shows: (i) a finite discontinuity, given by (18), when the point is elliptic; (ii) a logarithmic singularity, given by (26), when the point is hyperbolic; and (iii) an algebraic singularity, as in (30) or (33), when the point

is parabolic. [Note that our gross conclusions are not affected by the fact that the variety of the behaviours around parabolic points is richer than the two cases explicitly analysed.] The contributions to the asymptotic scattering amplitude, arising from the first two kinds of $\hat{\mathbf{q}}$ tangency points, were already worked out in §§2.1, 2.2, and are given by (20) and (27). To evaluate the contribution due to a parabolic $\hat{\mathbf{q}}$ tangency point, we need to evalute the leading term of the FTs of (30) and (33). To this aim, we note that both terms have the form

$$C\Theta[a(\delta-\xi)]|\delta-\xi|^{\lambda-1}, \tag{34}$$

and the explicit expressions of C and λ are obtained by comparing (34) with (30) or (33). In particular, $\lambda = 1/\alpha$ in the first case and $\lambda = 1/\alpha + 1/\beta$ in the second. Since both α and β are constrained to be larger than two [see (28)], then $0 < \lambda < 1$. Assume first that $a > 0$. Then, a parabolic $\hat{\mathbf{q}}$ point contributes to the Fourier integral on the r.h.s. of (16) with

$$\int_{-\infty}^{\delta} \mathrm{d}\xi \exp(iq\xi) C\Theta[a(\delta-\xi)](\delta-\xi)^{\lambda-1}.$$

According to the theorem reported by Erdélyi (1955, §2.8), the leading asymptotic term of this integral arises from the upper bound and is $C\Gamma(\lambda)\exp(-i\pi\lambda/2)\exp(iq\delta)/q^{\lambda}$. If $a < 0$, δ will be the lower bound of the integral, and the leading term reads $-C\Gamma(\lambda)\exp(i\pi\lambda/2)\exp(iq\delta)/q^{\lambda}$, which differs by a phase factor from that obtained in the case $a > 0$. To get the leading asymptotic contribution to the scattering amplitude (16), the previous two expressions must be divided by iq. One concludes that the leading asymptotic term due to a parabolic $\hat{\mathbf{q}}$ tangency is

$$\mathrm{sign}(a)C\Gamma(\lambda)\exp\{-i[\mathrm{sign}(a)\lambda+1]\pi/2\}\exp(iq\delta)/q^{\lambda+1}, \tag{35}$$

which is valid whatever the sign of a. A particle can have several elliptic, hyperbolic and parabolic $\hat{\mathbf{q}}$-tangency points, as well as planar subsets orthogonal to $\hat{\mathbf{q}}$. After labelling the points by indices $\imath$, $\jmath$ and ℓ and the planar subsets by j, and collecting the previous results, one finds the leading asymptotic expression of the geometrical scattering amplitude of the particle, namely

$$\mathcal{A}_p(q\hat{\mathbf{q}}) \approx \sum_{\imath} \mathcal{E}_{\imath} \frac{\exp(iq\delta_{\imath})}{q^2} + \sum_{\jmath} \mathcal{H}_{\jmath} \frac{\exp(iq\delta_{\jmath})}{q^2} + \sum_{\ell} \mathcal{P}_{\ell} \frac{\exp(iq\delta_{\ell})}{q^{1+\lambda_{\ell}}} + \sum_{j} \mathcal{S}_j \frac{\exp(iq\delta_j)}{q}. \tag{36}$$

The expressions for coefficients $\mathcal{E}_{\imath}$, $\mathcal{H}_{\jmath}$, $\mathcal{P}_{\ell}$ and $\mathcal{S}_j$ are obtained by comparing (36) with (18), (26), (35) and (16), respectively. By (27), the asymptotic behaviour of $\mathcal{A}_{\mathcal{V}_1}(q\hat{\mathbf{q}})$, the total scattering amplitude, is obtained after substituting each index of summation in (36) with a pair of indices, *e.g.* $\imath$ becomes $(p,\imath)$ where p labels the sample particles. Finally, the square modulus of this expression yields the asymptotic leading term of the scattering intensity. One finds

$$I(q\hat{\mathbf{q}}) \approx (\Delta n)^2 \Big[\sum_{p,\imath} \frac{|\mathcal{E}_{p,\imath}|^2}{q^4} + \sum_{p,\jmath} \frac{|\mathcal{H}_{p,\jmath}|^2}{q^4} + \sum_{p,\ell} \frac{|\mathcal{P}_{p,\ell}|^2}{q^{2+2\lambda_{p,\ell}}} + \sum_{p,j} \frac{|\mathcal{S}_{p,j}|^2}{q^2} \Big], \tag{37}$$

where only the contributions resulting from the product of each term with its complex conjugate have been retained. In fact, it is reasonable to expect that the sum of the cross terms, which are oscillatory, averages to zero for most of the samples. The $O(q^{-4})$ contributions of (37) can more compactly be written as

$$\frac{4\pi^2(\Delta n)^2}{q^4} \sum_{p,j} \frac{1}{|\kappa_{\mathrm{G},p,j}(\pm\hat{\mathbf{q}})|} \tag{38}$$

by equations (20), (27) and (16). In equation (38), the sum runs over all the points, labelled by (p,j), of the sample interface where the normal is equal to $\hat{\mathbf{q}}$ or to $-\hat{\mathbf{q}}$, and $|\kappa_{\mathrm{G},p,j}(\pm\hat{\mathbf{q}})|$ denotes the absolute value of the Gaussian curvature at the jth point of the pth particle. The $O(q^{-2})$ contribution takes the form

$$\frac{(\Delta n)^2 \sum_j S_j^2(\hat{\mathbf{q}})}{q^2}, \tag{39}$$

where $S_j(\hat{\mathbf{q}})$ denotes the area of the jth planar subset of the sample interface, orthogonal to $\hat{\mathbf{q}}$. The coefficients in front of the terms, asymptotically decreasing as $q^{-\lambda}$ with $2 < \lambda < 4$, are also related to the local structure of the interface, since they can be expressed in terms of coefficients a, b, α and so on, present in the local expansion (28*a*) of the surface. For instance, in the cylinder-like case, by combining (35) and (30) one has

$$|\mathcal{P}_{p,\ell}|^2 = \frac{4H^2\delta^{2(\alpha-1)/\alpha}\Gamma^2(1/\alpha)}{\alpha^2|a|^{2/\alpha}},$$

where, for notational simplicity, we avoided adding indices (p,ℓ) on the r.h.s.

4. Finite angular resolution and conclusion

In §3, we have obtained the general expression of the asymptotic leading term for anisotropic intensities along an arbitrary direction $\hat{\mathbf{q}}$ of reciprocal space. As these intensities refer to a precisely definite geometrical direction, they are not observable since the angular resolution is finite in any experiment. Consider a detector pixel under the (mean) scattering vector direction $\hat{\mathbf{q}}_0$ with an opening solid angle $\Delta\Omega(\hat{\mathbf{q}}_0)$ with respect to the sample position. The intensity collected by this pixel is

$$\bar{I}_{\Delta\Omega}(q\hat{\mathbf{q}}_0) = \int_{\Delta\Omega(\hat{\mathbf{q}}_0)} I(q\hat{\mathbf{q}})\,\mathrm{d}\hat{\mathbf{q}}. \tag{40}$$

Only the asymptotic analysis of $\bar{I}_{\Delta\Omega}(q\hat{\mathbf{q}}_0)$ is physically meaningful. To perform such an analysis, we need to know the asymptotic behaviour of $\bar{I}_{\Delta\Omega}(q\hat{\mathbf{q}}_0)$. This is obtained by substituting (37) in (40). If we consider first the $O(q^{-4})$ contributions, (40) becomes

$$\bar{I}_{\Delta\Omega}(q\hat{\mathbf{q}}_0) \approx \frac{4\pi^2(\Delta n)^2}{q^4}\sum_p \int_{\Delta\Omega(\hat{\mathbf{q}}_0)} \sum_\ell \frac{\mathrm{d}\hat{\mathbf{q}}}{|\kappa_{\mathrm{G},p\ell}(\pm\hat{\mathbf{q}})|}. \qquad (41)$$

According to a basic result of differential geometry (Smirnov, 1970), the value of the integral is the area of that part of the p particle surface which has its normals within the considered solid angle $\Delta\Omega(\hat{\mathbf{q}}_0)$. Denote this area by $S_p(\Delta\Omega(\hat{\mathbf{q}}_0))$. The total area of all the portions of the sample interface with the normals within $\Delta\Omega(\hat{\mathbf{q}}_0)$ is

$$S(\Delta\Omega(\hat{\mathbf{q}}_0)) = \sum_p S_p(\Delta\Omega(\hat{\mathbf{q}}_0)), \qquad (42)$$

and from (41) one gets

$$\bar{I}_{\Delta\Omega}(q\hat{\mathbf{q}}_0) \approx \frac{4\pi^2(\Delta n)^2 S(\Delta\Omega(\hat{\mathbf{q}}_0))}{q^4}. \qquad (43)$$

Equation (43) also holds in the presence of parabolic $\hat{\mathbf{q}}$ tangency points, provided these form a set with area equal to zero and $\kappa_{\mathrm{G}}^{-1}(\hat{\mathbf{q}})$ is an integrable function, these conditions ensuring the existence of the integral in (41). A simple example is the cuboidal particle discussed in Appendix *A*. In this case, the set of the parabolic $\hat{\mathbf{q}}$ tangency points consists of the three curves resulting from the intersections of the cuboidal surface with the three planes $x = 0$, $y = 0$ and $z = 0$. The area of this set is clearly zero since, as evident from (52), the order of the zeros of $\kappa_{\mathrm{G}}(\hat{\mathbf{q}})$ with respect to $\hat{q}_x$ and $\hat{q}_y$ is $[(\alpha-2)/(\alpha-1)] < 1$ on these lines. Thus, these singularities are integrable.

However, the presence of such singularities makes the value of $S(\Delta\Omega(\hat{\mathbf{q}}_0))$, relevant to a $\Delta\Omega(\hat{\mathbf{q}}_0)$ containing the directions associated with parabolic $\hat{\mathbf{q}}$ tangency points, larger than that relevant to a $\Delta\Omega(\hat{\mathbf{q}}_0)$ which does not contain such directions. These conclusions apply to any parabolic $\hat{\mathbf{q}}$ tangency point and one concludes that asymptotic terms decreasing as $q^{-\lambda}$, with $2 < \lambda < 4$, are not observable experimentally.

Finally, we discuss the contribution to $\bar{I}_{\Delta\Omega}(q\hat{\mathbf{q}}_0)$ resulting from the presence of planar facets on the sample interface. For simplicity, we refer to a cube. The leading asymptotic behaviour can be obtained by taking the limit $\alpha \to \infty$ of the asymptotic behaviour of the $\bar{I}_{\Delta\Omega}(q\hat{\mathbf{q}}_0)$ relevant to a cuboid with parameter α [see (46)]. Since $\bar{I}_{\Delta\Omega}(q\hat{\mathbf{q}}_0)$ asymptotically decreases as q^{-4} if α is finite (for a different proof of this property we refer to Appendix *B*), the Porod coefficient will be $4\pi^2(\Delta n)^2$ times the limit of $S_\alpha(\Delta\Omega(\hat{\mathbf{q}}_0))$ for $\alpha \to \infty$, where subscript α means that the quantity refers to the cuboid characterized by this parameter. Clearly, in the limit $\alpha \to \infty$, $S_\alpha(\Delta\Omega(\hat{\mathbf{q}}_0))$ becomes equal to the sum of the areas of the cube faces which have their normals within $\Delta\Omega(\hat{\mathbf{q}}_0)$. Thus, the Porod coefficient is still that reported on the r.h.s. of (43), but it should be noted that the smaller the size of the detector pixels the more sensitive the dependence of $S_\alpha(\Delta\Omega(\hat{\mathbf{q}}_0))$ on $\hat{\mathbf{q}}_0$. In the case of a cube, the observed asymptotic behaviour will be $O(q^{-4})$ only close to the directions orthogonal to the faces of the cube. Along other directions of reciprocal space, the decrease will be faster than q^{-4} and this fact explains the origin of the streaks often observed in anisotropic SAS intensities (see *e.g.* Kompatscher *et al.*, 2000). In conclusion, the generalization of Porod's law to anisotropic samples formed by particles of arbitrary shapes follows from (43) after dividing this equation by $\Delta\Omega(\hat{\mathbf{q}}_0)$ and reads

$$\frac{\bar{I}_{\Delta\Omega}(q\hat{\mathbf{q}}_0)}{\Delta\Omega(\hat{\mathbf{q}}_0)} \approx \frac{4\pi^2(\Delta n)^2 S(\Delta\Omega(\hat{\mathbf{q}}_0))}{q^4\Delta\Omega(\hat{\mathbf{q}}_0)}. \qquad (44)$$

With $\Delta\Omega(\hat{\mathbf{q}}_0) = 4\pi$, the left side of (44) is the isotropic component of the scattering intensity while $S(4\pi)$ is twice the area of the sample interface. In this way, Porod's law is recovered. When $\Delta\Omega(\hat{\mathbf{q}}_0) \ll 4\pi$, the definition of $S(\Delta\Omega(\hat{\mathbf{q}}_0))$, as the area of that part of the sample interface which has the normals within $\Delta\Omega(\hat{\mathbf{q}}_0)$, becomes important. In fact, the dependence of $S(\Delta\Omega(\hat{\mathbf{q}}_0))$ on $\hat{\mathbf{q}}_0$ can be observed, in favourable circumstances, from Porod plots of the intensity at various fixed $\hat{\mathbf{q}}_0$, with the result that the heights of the Porod plateaus will be higher (lower) along those directions where the interfaces are flatter (more bent).

APPENDIX *A*

Transmission electron microscopy of alloys that have undergone heat treatment often shows precipitates shaped as parallelepipeds with round edges tending to become sharper as particle growth proceeds. The surface of these particles is conveniently parametrized by the expression (Schneider *et al.*, 2000)

$$|x/a|^\alpha + |y/b|^\alpha + |z/c|^\alpha = 1 \qquad \text{with} \quad \alpha \geq 2. \qquad (45)$$

Here, a, b and c are the maximal half-lengths of a particle along axes x, y and z, while parameter α describes the roundness of the particles. In fact, (45) with $\alpha = 2$ is the equation of an ellipsoid with semi-axes a, b and c. As α increases, surface (45) tends to develop planar regions at the axis ends as well as edges of increasing sharpness. In the limit $\alpha \to \infty$, (45) reduces to $\{|x| = a, |y| < b, |z| < c\}$, $\{|x| < a, |y| = b, |z| < c\}$ and $\{|x| < a, |y| < b, |z| = c\}$, which are the equations of a right parallelepiped. Scaling coordinates x, y and z by a, b and c, we may convert (45) into

$$|x|^\alpha + |y|^\alpha + |z|^\alpha = 1. \qquad (46)$$

The shape of this surface will be called *cuboidal* and the particle *cuboid*. Equation (46) has a cubic symmetry, and can be studied in the region

$$0 \leq y \leq x \leq z. \qquad (47)$$

Here, (46) can uniquely be solved with respect to z. The solution reads

$$z = z(x, y) = (1 - x^\alpha - y^\alpha)^{1/\alpha}. \qquad (48)$$

Let $\mathbf{r}_1 = [x, y, z(x, y)]$ denote the position vector of a point of the cuboidal surface in region (47). At this point, the unit vector orthogonal to the cuboidal surface is

$$\hat{\mathbf{v}}(x, y) = \frac{1}{(EG - F^2)^{1/2}}[(x/z)^{\alpha-1}, (y/z)^{\alpha-1}, 1] \qquad (49)$$

and the Gaussian curvature reads

$$\kappa_G(x,y)=\frac{(\alpha-1)^2}{z^2(EG-F^2)^2}\left(\frac{xy}{z^2}\right)^{\alpha-2}\left[1+\frac{x^\alpha}{z^\alpha}+\frac{y^\alpha}{z^\alpha}\right]. \quad (50)$$

Expressions (49) and (50) are given in terms of the Cartesian coordinates of the point. The coordinates of the point of the cuboidal surface where $\hat{\mathbf{v}}=\hat{\mathbf{q}}$, $\hat{\mathbf{q}}$ being an arbitrary unit vector, are easily determined as follows. [For simplicity, we assume that $\hat{\mathbf{q}}$ lies in the angular sector defined by (47). The other cases are recovered by an appropriate permutation of coordinates and changes of signs.] By (49), the requirement $\hat{\mathbf{v}}=\hat{\mathbf{q}}$ can be written as

$$[(x/z)^{\alpha-1},(y/z)^{\alpha-1},1]=\lambda\hat{\mathbf{q}}=\lambda(\hat{q}_x,\hat{q}_y,\hat{q}_z),$$

where $\lambda=(EG-F^2)^{1/2}$. In this way, one gets

$$\lambda=\hat{q}_z^{-1},\quad x=z\left(\frac{\hat{q}_x}{\hat{q}_z}\right)^{1/(\alpha-1)},\quad y=z\left(\frac{\hat{q}_y}{\hat{q}_z}\right)^{1/(\alpha-1)}.$$

After substituting these expressions of x and y in (48), the coordinates of the point of the surface where $\hat{\mathbf{v}}=\hat{\mathbf{q}}$ are

$$x=\frac{\hat{q}_x^{1/(\alpha-1)}}{D^{1/\alpha}},\quad y=\frac{\hat{q}_y^{1/(\alpha-1)}}{D^{1/\alpha}},\quad \text{and}\quad z=\frac{\hat{q}_z^{1/(\alpha-1)}}{D^{1/\alpha}}, \quad (51a-c)$$

where

$$D\equiv[\hat{q}_x^{\alpha/(\alpha-1)}+\hat{q}_y^{\alpha/(\alpha-1)}+\hat{q}_z^{\alpha/(\alpha-1)}]. \quad (51d)$$

The substitution of (51*a–d*) into (50) yields the following expression for the Gaussian curvature in terms of $\hat{\mathbf{q}}$:

$$\kappa_G(\hat{\mathbf{q}})=(\alpha-1)^2D^{(\alpha+2)/\alpha}(\hat{q}_x\hat{q}_y\hat{q}_z)^{(\alpha-2)/\alpha-1}. \quad (52)$$

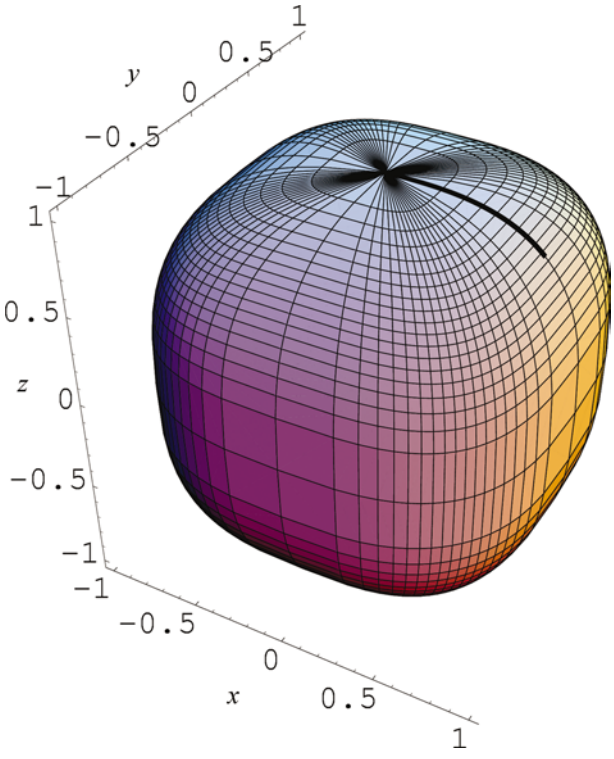

Figure 3
Visualization of the cuboidal particle defined by equation (46) with $\alpha=3$. In the figure, the bold arc is the arc PQ referred to in the text with its left end P lying at the top of the surface.

Equations (52) and (38) allow us to get the leading term expression of the scattering intensity of a cuboid along the directions of reciprocal space where (52) is not equal to zero. For completeness, we work out the leading terms along the 'singular' directions, *i.e.* the values of $\hat{\mathbf{q}}$ where $\kappa_G(\hat{\mathbf{q}})=0$. From (50), it immediately follows that, in the region (47), κ_G is equal to zero at the points having position vectors

$$\mathbf{r}_1=(x,0,z(x,0))\quad\text{with}\quad 0\le x\le 2^{-1/\alpha},$$

and forming the arc PQ shown in Fig. 3. In order to determine the behaviour of $A'_{p,C}(\xi,\hat{\mathbf{q}})$ around these points, it is first noted that point P must be analysed separately from the other points lying on the arc PQ. In fact, the order of the zero of κ_G is $2(\alpha-2)$ at P, and $(\alpha-2)$ at the remaining points of PQ. At $P=(0,0,1)$, one has $\hat{\mathbf{q}}\equiv\hat{\mathbf{q}}_0=(0,0,1)$. From (48), it follows that $\hat{\mathbf{q}}_0\cdot\mathbf{r}\approx 1-(x^\alpha+y^\alpha)/\alpha$, which, in a complete neighbourhood of P, becomes

$$\hat{\mathbf{q}}_0\cdot\mathbf{r}\approx 1-(|x|^\alpha+|y|^\alpha)/\alpha.$$

Its comparison with (28*a*) shows that we are in the case $2\le\alpha\le\beta$ with $a=b=1/\alpha$ (and $ab>0$). By result (33), the leading behaviour of $A'_{p,C}(\xi,\hat{\mathbf{q}}_0)$ is

$$A'_{p,C}(\xi,\hat{\mathbf{q}}_0)\approx-\frac{4\Theta(\zeta)\Gamma^2(1/\alpha)\alpha^{(2-2\alpha)/\alpha}}{\Gamma(2/\alpha)\zeta^{1-2/\alpha}}. \quad (53)$$

Furthermore, for the remaining points of PQ, we need to expand (48) around $(x_0,0)$ with $x_0\neq 0$. Thus, setting $x=x_0+X$ and $y=Y$, (48) becomes

$$z=[1-x_0^\alpha(1+X/x_0)^\alpha-|Y|^\alpha]^{1/\alpha}.$$

Expanding around $(x_0,0)$ and recalling that $z_0=[1-x_0^\alpha]^{1/\alpha}$, one finds

$$z\approx z_0\left\{1-\left(\frac{x_0}{z_0}\right)^\alpha\frac{X}{x_0}-\frac{\alpha-1}{2}\left(\frac{x_0}{z_0}\right)^\alpha\left[1+\left(\frac{x_0}{z_0}\right)^\alpha\right]\left(\frac{X}{x_0}\right)^2-\frac{1}{\alpha}\left(\frac{|Y|}{z_0}\right)^\alpha+\ldots\right\}. \quad (54)$$

From (54), it follows that

$$\mathbf{r}\cdot\hat{\mathbf{q}}\approx\delta-aX^2-b|Y|^\alpha+\ldots \quad (55)$$

with $\delta=\hat{q}_xx_0+\hat{q}_zz_0$ and

$$a\equiv\frac{\hat{q}_z(\alpha-1)}{2z_0}\left(\frac{x_0}{z_0}\right)^{\alpha-2}\left[1+\left(\frac{x_0}{z_0}\right)^\alpha\right] \quad (56a)$$

$$b=\hat{q}_z/\alpha z_0^{\alpha-1}. \quad (56b)$$

From (55), one gets

$$\Xi=\mathbf{r}\cdot\hat{\mathbf{q}}-\xi\approx\zeta-aX^2-b|Y|^\alpha.$$

The comparison of this expression with (31) yields $\alpha=2$, $\beta=\alpha$. Substituting these values in (33) yields the leading term of $A'_{p,C}(\xi,\hat{\mathbf{q}})$ around the points lying on the arc $[PQ]$, *i.e.*

$$A'_{p,C}(\xi,\hat{\mathbf{q}})\approx-\frac{2\Theta(\zeta)\Gamma(1/2)\Gamma(1/\alpha)}{\alpha|a|^{1/2}|b|^{1/\alpha}\Gamma(1/2+1/\alpha)\zeta^{(\alpha-2)/2\alpha}}. \quad (57)$$

Here, a and b are given by (56*a*) and (56*b*), and they can be expressed in terms of $\hat{\mathbf{q}}$ by (51*a–d*). In conclusion, (53) refers to the directions defined by the axes of the cuboid, while (57)

applies to the remaining directions contained in the three 'equatorial' sections (reminder of the cubic symmetry of the particle). Writing (53) and (57) in the form (34) and using relations (35) and (37), one finds that the leading term of the form factor of a cuboid is

$$I(q\hat{\mathbf{q}}_0) \approx \frac{32(\Delta n)^2\alpha^{4(1-\alpha)/\alpha}\Gamma^4(1/\alpha)}{q^{2(1+2/\alpha)}} \tag{58}$$

along the axes of reciprocal space and

$$I(q\hat{\mathbf{q}}) \approx \frac{8(\Delta n)^2\Gamma^2(1/2)\Gamma^2(1/\alpha)}{\alpha^2|a||b|^{2/\alpha}q^{3+2/\alpha}}, \tag{59}$$

along the other singular directions. It is noted that the exponents of q in (58) and (59) span the intervals [2, 4] and [3, 4], respectively, as α ranges in [2, ∞].

APPENDIX *B*

A different proof is now given of the property that the leading asymptotic term of the scattering intensity of a homogeneous cube, after being integrated on a small solid angle centred on the direction orthogonal to one of the faces, is $O(q^{-4})$. The scattering intensity from a cube with edges of unit length, faces along the Cartesian planes and scattering contrast equal to one is

$$F(\mathbf{q}) = \prod_{j=1}^{3}\left[\frac{\sin(q_j/2)}{q_j/2}\right]^2 = 8\prod_{j=1}^{3}\frac{1-\cos(q_j)}{q_j^2}, \tag{60}$$

where q_1 is the component of $\mathbf{q}$ along the x axis and so on. Take now $\hat{\mathbf{q}}_0 = (0, 0, 1)$. From (60), it follows that

$$F(q\hat{\mathbf{q}}_0) = \frac{2(1-\cos\, q)}{q^2}, \tag{61}$$

so that $F(q\hat{\mathbf{q}}_0)$ asymptotically behaves as predicted by (39). Integrating $F(\mathbf{q})$ on a small solid angle having $\hat{\mathbf{q}}_0$ as symmetry axis and $2\theta_0$ as opening angle yields

$$\bar{F}_{\Delta\Omega(\hat{\mathbf{q}}_0)}(q\hat{\mathbf{q}}_0) \equiv \frac{64}{q^6}\int_0^{\theta_0}\sin\theta\,\mathrm{d}\theta\int_0^{\pi/4}\mathrm{d}\varphi\left[\frac{1-\cos(q\cos\theta)}{\cos^2\theta}\right] \times \frac{[1-\cos(q\sin\theta\cos\varphi)][1-\cos(q\sin\theta\,\sin\varphi)]}{\sin^4\theta\cos^2\varphi\sin^2\varphi}. \tag{62}$$

In terms of the new integration variables X and Y,

$$X = q\sin\theta\cos\varphi \tag{63a}$$

$$Y = q\sin\theta\sin\varphi, \tag{63b}$$

(62) becomes

$$\frac{32}{q^4}\int_R \mathrm{d}X\,\mathrm{d}Y\left[\frac{1-\cos X}{X^2}\right]\left[\frac{1-\cos Y}{Y^2}\right] \times \left[\frac{1-\cos\{q[1-(X^2+Y^2)/q^2]^{1/2}\}}{[1-(X^2+Y^2)/q^2]^{3/2}}\right], \tag{64}$$

where R denotes the portion of the circle $X^2 + Y^2 \le q^2\sin^2\theta_0$ contained in the first quadrant of plane XY. Each expression inside the large square brackets of (64) is continuous and non-negative. [This is true also for the last factor owing to the constraint on the variables.] By the second theorem of the mean for integrals, (64) becomes

$$\frac{32C(q,\theta_0)}{q^4}\int_R \mathrm{d}X\,\mathrm{d}Y\left[\frac{1-\cos X}{X^2}\right]\left[\frac{1-\cos Y}{Y^2}\right] \tag{65}$$

with

$$C(q,\theta_0) \equiv \left[\frac{1-\cos\{q[1-(\bar{X}^2+\bar{Y}^2)/q^2]^{1/2}\}}{[1-(\bar{X}^2+\bar{Y}^2)/q^2]^{3/2}}\right], \tag{66}$$

$(\bar{X}, \bar{Y})$ being a suitable point internal to R and continuous on q and θ_0. The first condition ensures that $0 < (\bar{X}^2 + \bar{Y}^2) \le q^2\cos^2\theta_0$ so that $C(q, \theta_0)$ cannot diverge. Thus, the factor in front of integral (65) cannot decrease more slowly than q^{-4}. However, coefficient $C(q, \theta_0)$ cannot tend to zero as $q \to \infty$ because the denominator cannot diverge or the square root in the argument of the cosine function cannot approach zero owing to the reported constraint on $(\bar{X}^2 + \bar{Y}^2)$. Thus, (65) at large q behaves as q^{-4} if the integral is finite and different from zero. This property is easily proved observing that each factor of the integrand is non-negative and that the integration domain increases with q. By the first condition, the integral must be strictly positive and by the second its value is smaller than that obtained by letting $R \to \infty$. Hence,

$$\int_R \mathrm{d}X\,\mathrm{d}Y\left[\frac{1-\cos X}{X^2}\right]\left[\frac{1-\cos Y}{Y^2}\right] < \left[\int_0^{\infty}\mathrm{d}X\left(\frac{1-\cos X}{X^2}\right)\right]^2 = (\pi/2)^2,$$

where the last equality is obtained by the residue theorem. Combining this result with (65), one concludes that

$$\bar{F}_{\Delta\Omega(\hat{\mathbf{q}}_0)}(q\hat{\mathbf{q}}_0) \approx (8\pi^2/rq^4)C(q,\theta_0).$$

In conclusion, the angular average of the form factor of a cube over a small solid angle centred on a 'singular' $\hat{\mathbf{q}}$ direction yields an $O(q^{-4})$ behaviour.

SC is grateful to the Institut für Angewandte Physik of the ETH-Zürich, where this work was carried out, for a visiting professorship and to all its members for stimulating discussions.

References

Ciccariello, S. (1997). *X-ray Investigations of Polymer Structures*, edited by A. Wlochowicz. *SPIE*, Vol. 3095, pp. 142–156.
Ciccariello, S., Schneider, J.-M., Schönfeld, B. & Kostorz, G. (2000). *Europhys. Lett.* **50**, 601–607.
Debye, P., Anderson, H. R. & Brumberger, H. (1957). *J. Appl. Phys.* **28**, 679–683.
Erdélyi, A. (1955). *J. Soc. Ind. Appl. Math.* **3**, 17–24.
Erdélyi, A. (1958). *Asymptotic Expansions.* Dover: New York.
Feigin, I. A. & Svergun, D. I. (1987). *Structure Analysis by Small-Angle X-ray and Neutron Scattering.* New York: Plenum Press.
Glatter, O. & Kratky, O. (1982). *Small-Angle X-ray Scattering.* London: Academic Press.

Gradshtein, I. S. & Ryzhik, I. M. (1980). *Tables of Integrals, Series and Products.* London: Academic Press.
Guelfand, I. M. & Chilov, G. E. (1962). *Les Distributions*, Vol. I, ch. 3. Paris: Dunod.
Guinier, A. & Fournet, G. (1955). *Small-Angle Scattering of X-rays*. New York: Wiley.
Jones, D. S. & Kline, M. (1958). *J. Math. Phys. (Mass.)* **37**, 1–54.
Kompatscher, M., Schönfeld, B., Heinrich, H. & Kostorz, G. (2000). *J. Appl. Cryst.* **33**, 488–491.
Kostorz, G. (1996). *Physical Metallurgy*, edited by R. W. Cahn & P. Haasen, Vol. I, ch. 12. Amsterdam: North-Holland.
Lindner, P. & Zemb, Th. (1991). *Neutron, X-ray and Light Scattering.* Amsterdam: North-Holland.
Luzzati, V., Witz, J. & Nicolaieff, A. (1961). *J. Mol. Biol.* **3**, 367–370.
Martin, J. E. & Hurd, J. A. (1987). *J. Appl. Cryst.* **20**, 61–75.
Porod, G. (1951*a*). *Kolloid Z.* **124**, 83–114.
Porod, G. (1951*b*). *Kolloid Z.* **125**, 51–57.
Ruland, W. (1971). *J. Appl. Cryst.* **4**, 70–73.
Schneider, J.-M., Schönfeld, B., Demé, B. & Kostorz, G. (2000). *J. Appl. Cryst.* **33**, 465–468.
Smirnov, V. (1970). *Cours de Mathématiques Supérieures*, Vol. II, ch. V.2. Moscow: MIR.